

Multistability and Control in Ring Networks of Phase Oscillators with Frequency Heterogeneity and Phase Delay

Soomin Kim^{1, a)} and Hiroshi Kori^{1, b)}

Graduate School of Frontier Sciences, The University of Tokyo, Chiba 277-8561, Japan

(Dated: 18 February 2025)

Many oscillator networks are multistable, meaning that different synchronization states are realized depending on the initial conditions. In this paper, we numerically analyze a ring network of phase oscillators, in which synchronous states with different wavenumbers are simultaneously stable. This model is an extension of the one studied in detail in previous studies by introducing inhomogeneities in the natural frequencies and the phase delay in the interaction, which are essential factors in the application. We investigate basin size distribution, which characterizes the size of the initial value set that converges to each synchronous state, showing that the basin size of synchronous states with higher wavenumbers broadens as the phase delay increases up to a certain extent. Weak inhomogeneities in the natural frequencies are also found to broaden the basin size of synchronous states with lower wave-numbers, i.e., more synchronous states. The latter result is seemingly counter-intuitive, but occurs because the higher wavenumber states are more vulnerable to inhomogeneity. Finally, we propose a control method that exploits inhomogeneity and phase delay to steer the system into a synchronized state with a specific wavenumber. This research furthers our understanding of the design principles and control of oscillator networks.

Synchronization of oscillator networks is crucial for a system to function properly. For instance, the heart, which pumps blood, and the central pattern generator, the neural tissue controlling motor activities like breathing and walking in animals, only operate effectively when groups of cardiac or nerve cells are synchronized in the correct pattern. Oscillator networks are often multistable. That is, the system may converge to different synchronization states depending on initial conditions, or it may transition from one synchronization state to another upon perturbation. With multistability, a single oscillator network can realize different functions. In some species, it has been reported that central pattern generators utilize multistability to achieve different motions. On the other hand, arrhythmia states exist in the heart as stable states. A severe one is the ventricular fibrillation, which can lead to death if the heart transitions to this state for any reason. Generally speaking, if there is only one desired synchronization state, the oscillator network should be designed such that this state is the only stable one. If there is more than one desirable synchronization state, or if undesirable synchronization states cannot be eliminated, then control methods are required to guide the system to the desired synchronization state. These are challenging problems that inherently involve system nonlinearities. It is expected that a better understanding of systems with moderate complexity will provide hints for clarifying these principles. Against this background, this study investigates multistability in detail using a simple oscillator network, and proposes a control method based on the findings obtained. Novel results were obtained, such as the fact that system heterogeneity can be used to monostabilize and control the system.

I. INTRODUCTION

Various natural and artificial systems are composed of a population of individual units forming a network. Especially when those units are oscillators, it is known that those units interact with each other and show collective behavior called synchronization¹⁻⁴. Synchronization has been observed in a wide variety of system such as group of fireflies⁵, chorus of frogs⁶, firing in neurons⁷, and power grids⁸.

Synchronization is essential for proper functioning of oscillator networks. The required synchronization patterns vary depending on the target and situation. For example, the heart functions as a pump by having numerous cardiac muscle cells beat in a nearly in-phase synchronization pattern. However, the heart can enter a dynamic state with a complex spatial pattern known as ventricular fibrillation, which can lead to loss of function and death⁹. Thus, the heart is a multistable system with undesirable synchronization patterns. In contrast, the situation is different in locomotion. Many animals exhibit multiple gaits, generated by neural networks known as central pattern generators (CPGs)¹⁰. The synchronization patterns of CPGs are believed to switch flexibly through inputs from the central nervous system and feedback from external sensory inputs¹¹. Therefore, CPGs can also be considered multistable systems in a broad sense.

The multistability of oscillator networks has been extensively studied. Among oscillator networks that exhibit multistability, a particularly simple model is a ring network of phase oscillators. Canavier et al. considered a small ring network as a model of CPG, reporting on multistability and control methods¹². Wiley and Strogatz numerically investigated a large ring network to find that the basin size distribution is Gaussian¹³. The validity of this distribution was further examined^{14,15}. Although the ring network is simple and common, the multistable structure in ring networks is surprisingly complex, making them a useful model for understanding the multistability of oscillator networks.

One of the ultimate goals in the study of oscillator networks

^{a)}Electronic mail: thruminkim@gmail.com

^{b)}Electronic mail: kori@k.u-tokyo.ac.jp

is to elucidate the design principles of synchronization patterns and to develop control methods. How can we make the desired ordered state more stable, or even monostable? What are the control methods to converge a multistable system to a specific attractor? By deepening our understanding of specific systems and achieving these goals within those systems, we may be able to grasp clues to general principles.

In this study, we investigate the dynamical properties of a ring network of phase oscillators, following previous research, and propose control methods. To incorporate important factors in oscillator networks, we extend those used in previous studies by introducing frequency heterogeneity and generalizing the interaction function. The former is essential, especially when considering applications to natural systems such as biological and chemical systems. The latter specifically involves introducing an interaction function with a phase delay used in the Sakaguchi-Kuramoto model¹⁶. The motivation for this is that the phase delay in the interaction function plays an essential role in the entrainment and wave formation in spatially extended systems¹⁷. These factors, in fact, have been found to have a significant impact on the dynamical properties, including multistability and basin size. Finally, based on the revealed dynamical properties, we propose a control method to drive the system into a target synchronization pattern.

II. MODEL

Our study is motivated by a predecessors work by Wiley and Strogatz¹³. They investigated a ring network of N identical phase oscillators, each coupled with l neighbors on both sides. Specifically, the dynamical equation is given as

$$\dot{\phi}_k = \omega + \sum_{j=i-l}^{i+l} \sin(\phi_j - \phi_k), \quad (1)$$

where ω and ϕ_k is the frequency and the phase of oscillator i ($i = 1, 2, \dots, N$), respectively, and $\phi_{k+mN} = \phi_k$ for $m = \pm 1, \pm 2, \dots$. We may set $\omega = 0$ without loss of generality because this treatment is equivalent to the variable change $\phi_k \rightarrow \phi_k - \omega t$ for $i = 1, 2, \dots, N$. By substituting Eq. (2) into Eq. (1), one can confirm that this system has the following synchronized states:

$$\phi_k = \Omega t + \frac{2\pi q i}{N} + C, \quad (2)$$

where Ω is the synchronized frequency, C is an arbitrary constant, and q ($-\frac{N}{2} < q \leq \frac{N}{2}$) is an integer called a winding number. When k is regarded as a spatial axis, the wavenumber of the state is given as $2\pi q$. In this particular model, we have $\Omega = \omega$. The state with q is referred to as the uniformly q -twisted state. Some examples are shown in Fig. 1. We also refer to the state with $q = 0$ as the in-phase state. Wiley and Strogatz defined the size of the basin of each q -twisted state as the probability that the system converges to the q -twisted state from fully random initial conditions.

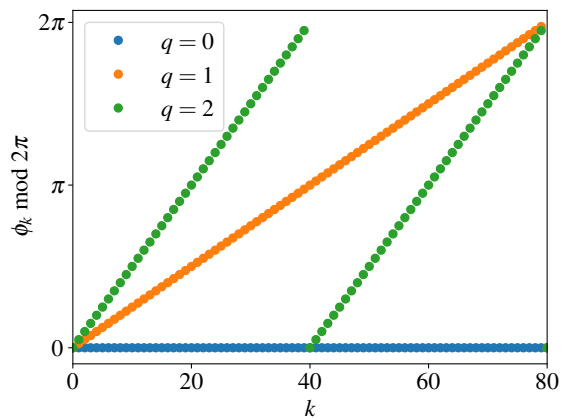


FIG. 1. Examples of the uniformly twisted states given by Eq. (2). The wavenumber of the q -twisted state is $2\pi q$.

In this study, as a variant of the original model (1), we consider

$$\dot{\phi}_k = \omega_k + \sin(\phi_{k-1} - \phi_k + \alpha) + \sin(\phi_{k+1} - \phi_k + \alpha). \quad (3)$$

where ω_k is the natural frequency of oscillator i and α is the phase offset in the interaction function. For $\omega_k = \omega$ for $i = 1, \dots, N$, we have the homogeneous q -twisted states, given by Eq. (2), where $\Omega = \omega + 2 \sin \alpha \cos(\frac{2\pi q}{N})$. The phase oscillators with this particular interaction function is first consider by Sakaguchi and Kuramoto¹⁷. It is well known that α significantly affects synchronization properties and nonzero α is responsible for the generation of wave patterns in the presence of a pacemaker region in spatially extended systems^{2,17,18}. Therefore, we expect that the basin size distribution depends critically on α . Natural frequency ω_k follows the normal distribution $\mathcal{N}(\omega, \sigma^2)$. The mean does not affect synchronization properties at all and is set to $\omega = 0$ without loss of generality. In contrast, the effect of σ is significant. For example, if σ is sufficiently large, oscillators with natural frequencies that deviate considerably from the mean will be not synchronized. If the distribution is sufficiently narrow, all oscillators will be synchronized. Even in this case, the basin size distribution may depend on σ . For simplicity, we focus on $k = 1$ and do not investigate the effect of non-local coupling; i.e., $l \geq 2$ in Eq. (1) in this study.

III. NUMERICAL ANALYSIS

We conduct numerical simulation of Eq. (3) with $N = 80$ to reveal the dynamical properties. We only consider the parameter region of α in which the in-phase state (i.e., the q -twisted state with $q = 0$) is stable in the absence of frequency heterogeneity ($\sigma = 0$). As details in Appendix A, such a region is $-\frac{\pi}{2} < \alpha < \frac{\pi}{2}$. Within this region, the q -twisted state with $|q| < \frac{N}{2}$ is stable. Furthermore, because the model is invariant under $\phi_k \rightarrow -\phi_k$, $\omega_k \rightarrow -\omega_k$ and $\alpha \rightarrow -\alpha$, the synchronization properties are expected to be the same for positive and negative α values for a large ensemble of frequency distributions. Therefore, we further limit ourselves to consider $0 \leq \alpha < \frac{\pi}{2}$.

A. Basin sizes

We first focus on the size of the basin of phase-locking states. In each run of simulation, we randomly and independently set ω_k and $\phi_k(0)$ for $i = 1, \dots, N$, following the normal distribution $\mathcal{N}(0, \sigma^2)$ and the uniform distribution in the range $[0, 2\pi)$, respectively. We then run a numerical simulation for $0 \leq t \leq 10^5$. Convergence to a phase-locking state is judged using Kuramoto order parameter $r(t) = \frac{1}{N} |\sum_{j=1}^N e^{i\phi_j}|$. When $|r(t+1) - r(t)| < 10^{-7}$, we judge that the convergence occurs and terminate the simulation. In this case, we calculate the winding number q by

$$q = \frac{1}{2\pi} \sum_{k=1}^N \psi_k, \quad (4)$$

where $\psi_k = \phi_{k+1} - \phi_k$ for $i = 1, \dots, N-1$ and $\psi_N = \phi_N - \phi_1$, which are defined in the range $(-\pi, \pi]$. We repeat this for $M = 10^5$ times to obtain the distribution of realized q .

In Fig. 2(a), we show the number of cases in which the system converges to a phase-locking state for given parameter values. We observe that for small σ , the system converges to a phase-locking state for all or most runs. As σ increases, the convergence occurs less likely, as naturally expected. We also observe that convergence is facilitated and impeded as α increases for $0 \leq \alpha \lesssim 0.25\pi$ and $0.25\pi \lesssim \alpha \leq 0.45\pi$, respectively. The system synchronizes most robustly for $\alpha \simeq 0.20$.

We next focus on the distribution of the winding number q of obtained phase-locking states. Figure 3(a), which is for different α values with fixed $\sigma = 0$, shows that the distribution becomes wider as α increases while keeping its unimodality. This property holds approximately true for $\sigma > 0$ (result not shown). This indicates that convergence to a twisted state with larger $|q|$ values is facilitated as α increases. On the other hand, the σ dependency is rather complicated. For $\alpha = 0$, as shown in 3(b), the distribution becomes narrower as σ increases. This suggests that the frequency heterogeneity breaks the states with large $|q|$ values. For $\alpha = 0.3\pi$, as shown in Fig. 3(c), a similar tendency is observed for $\sigma \leq 0.2$, but for $\sigma > 0.2$, conversely, the distribution becomes wider as σ increases. In any cases, the distributions look like Gaussian; this property seems robust against the frequency heterogeneity and the phase delay in the interaction function. As a summary, we show the standard deviation the q distribution for each parameter set (α, σ) in Fig. 2(b). We can confirm that the standard deviation increases as α increases for any σ values, whereas the dependence on σ is not necessarily monotonous.

We expect that $\sigma_c(q)$ and $\sigma_c(-q)$ coincides if we have a large number of samples. Therefore, we consider only $q \geq 0$. We observe that σ_c increases and decreases as α increases for $\alpha = 0, 0.1\pi, 0.2\pi$ and for $\alpha = 0.3\pi, 0.4\pi$, respectively. This indicates that the existence of the stable q -twist state is strongly dependent on α and facilitate it up to $\alpha \simeq 0.2\pi$. We also observe that whereas the state with $q = 0$ is most robust against the frequency heterogeneity for $\alpha = 0$, the q value corresponds to the most robust q -twisted state increases with α . These properties are consistent with the basin distribution shown in Figs. 3(b) and (c). We interpret that for $\alpha = 0$,

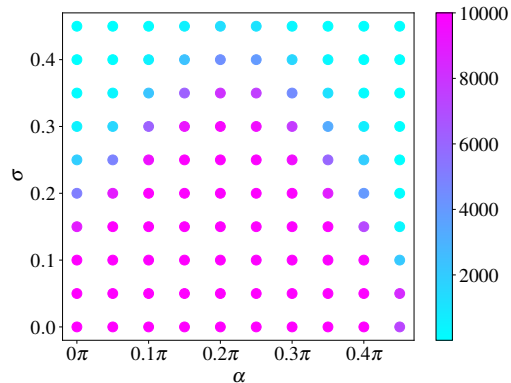


FIG. 2. The number of cases in which the system converges to a phase-locking state out of 10^5 runs of simulation.

shown in Fig. 3(b), the frequency heterogeneity tends to eliminate twisted states with larger $|q|$ values more than those with smaller $|q|$ values, and, thus, the basin of the twisted states with small $|q|$ increases. In contrast, for $\alpha = 0.3\pi$, shown in Fig. 3(c), twisted states with small $|q|$ values tends to be eliminated as σ increases, and, thus, the basin of the twisted states with small $|q|$ decreases.

B. Robustness of twisted states against the frequency heterogeneity

To understand the effect of the frequency heterogeneity on the multi-stability, we measure the critical σ values, denoted as $\sigma_c(q)$, above which the stable q -twisted state no more exist. The procedure to obtain $\sigma_c(q_1)$ is as follows. We first generate a frequency set, $\{\hat{\omega}_k\}$ ($i = 1, \dots, N$), from the normal distribution $\mathcal{N}(0, 1)$ and set $\{\omega_k\} = \{\sigma \hat{\omega}_k\}$. The initial condition is given by the uniformly twisted state, Eq. (2), for $q = q_1$. We then run a simulation for $\sigma = \Delta\sigma$, where $\Delta\sigma = 0.01$. If the system converges to a phase-locked state and the obtained q value is the same as q_1 , we increase σ by $\Delta\sigma = 0.01$ and run a simulation without resetting the θ_k values. Otherwise, the current σ value gives $\sigma_c(q_1)$. In Fig. 4, we plot $\sigma_c(q)$ for three different frequency sets with (a) $\alpha = 0$ and (b) 0.1π . We observe that $\sigma_c(q)$ is unimodal and peaked at different q values. Comparing $\alpha = 0$ and 0.1π cases, the latter tends to has a maximum $\sigma_c(q)$ at a larger q value. In Fig. 5, we plot the mean and the standard deviation of $\sigma_c(q)$ obtained from 100 different sets of $\{\hat{\omega}_k\}$. We observe that σ_c increases and decreases as α increases for $\alpha = 0, 0.1\pi, 0.2\pi$ and for $\alpha = 0.3\pi, 0.4\pi$, respectively. Thus, the phase delay up to some extent makes the synchronization robust against frequency heterogeneity. For $\alpha = 0$, the maximum $\sigma_c(q)$ is located at $q = 0$, which is the nearly in-phase state. This indicates that, as heterogeneity is increased, states with larger values of q tend to disappear earlier, and, statistically, the nearly in-phase state is most robust against the frequency heterogeneity. This result is consistent with the result shown in Fig. 3(a), in which large heterogeneity promotes the convergence to the nearly in-phase state. For $\alpha > 0$, the maximum $\sigma_c(q)$ is located at $|q| > 0$, thus the

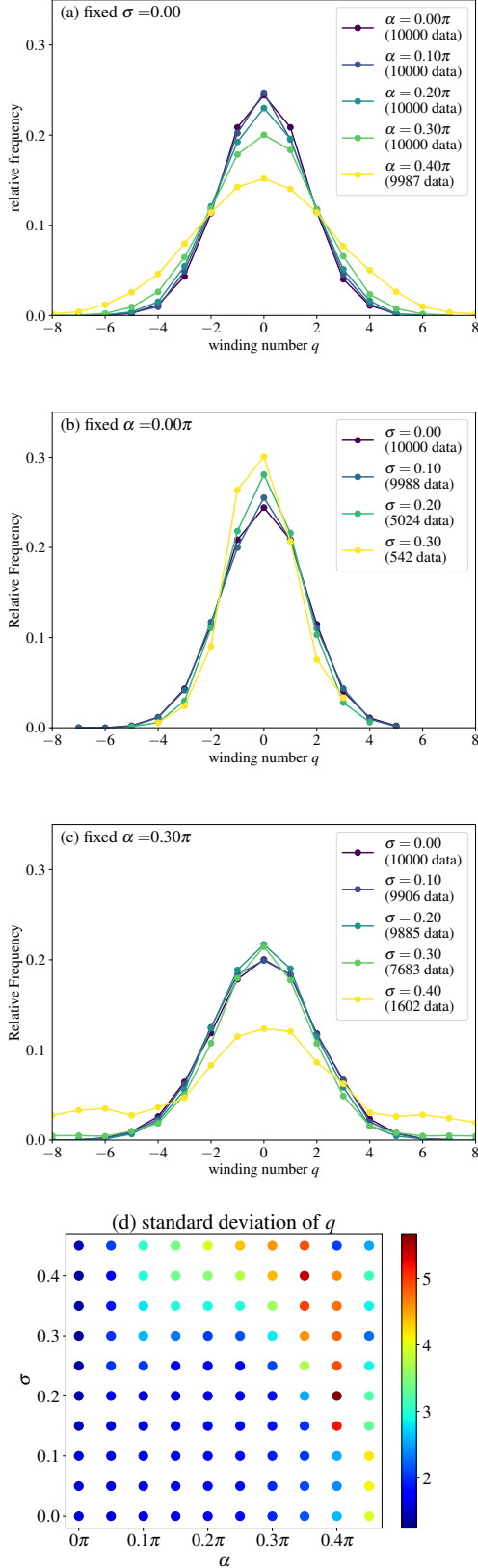


FIG. 3. The basin size distribution of the q -twisted states for (a) different α values with fixed $\sigma = 0$ and (b, c) different σ values with fixed $\alpha = 0$ and 0.3π , respectively. (d) The standard deviation of the q distribution as a function of α and σ .

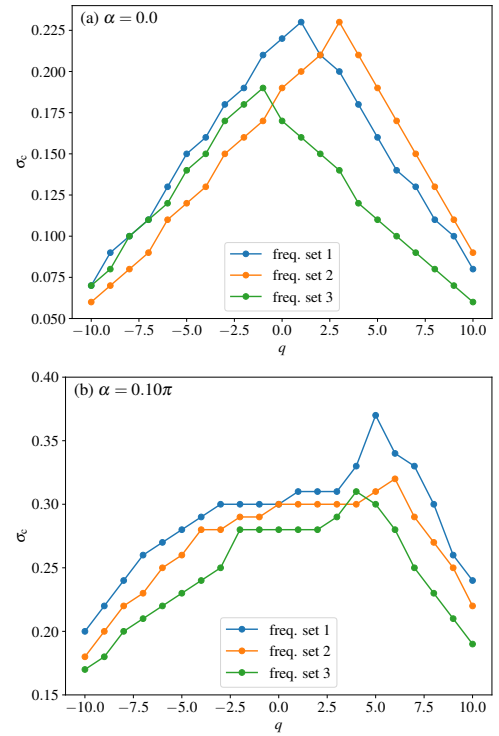


FIG. 4. Critical $\sigma_c(q)$ of each q -twisted state for three frequency sets. (a) $\alpha = 0$. (b) $\alpha = 0.1\pi$.

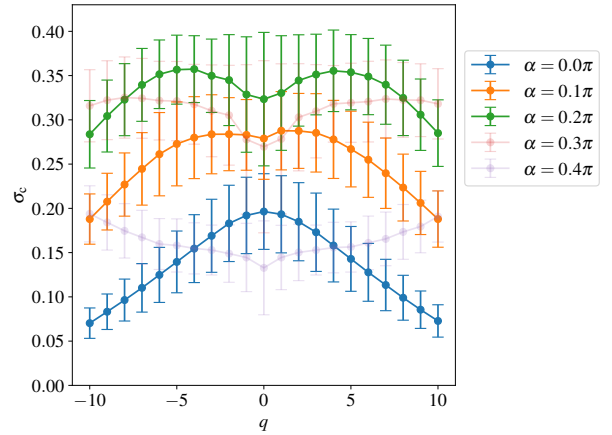


FIG. 5. The mean and the standard deviation of $\sigma_c(q)$ obtained for 100 frequency sets.

frequency heterogeneity promotes the convergence to twisted states with larger $|q|$ values.

C. Control

The result shown in Fig. 4 suggests a method to steer the system to a specific twisted state without directly manipulating the state variables. Figure 4 indicates that there exists specific frequency set and values of α and σ_c in which a sole q -twisted state becomes an attractor among all phase-locked states. Thus, by choosing such parameter values, the system

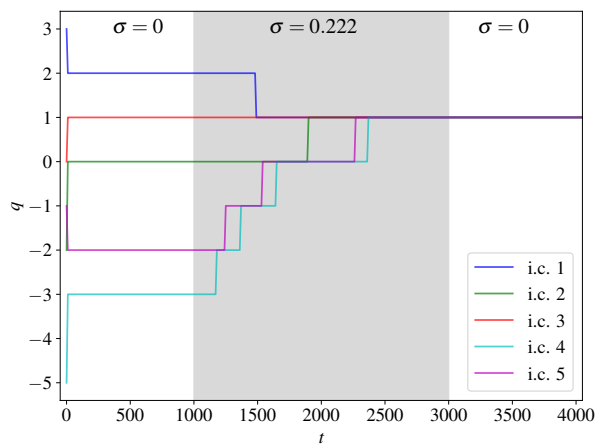


FIG. 6. The time-series of q for 5 different random initial conditions, in which $\sigma = 0.222$ for $1000 \leq t \leq 3000$ and $\sigma = 0$ otherwise.

will converge to a target q -twisted state for any initial conditions under the assumption that only the phase-locked states are possible attractors of the system. As an example, we demonstrate this idea using the frequency set 1 with $\alpha = 0$. With this, as seen in Fig. 4(a), the twisted state with $q = 1$ becomes monostable for $0.220 \lesssim \sigma \lesssim 0.225$. In Fig. 6, we show the time-series of q for 5 different random initial conditions, in which $\sigma = 0.222$ for $1000 \leq t \leq 3000$ and $\sigma = 0$ otherwise. Various q -twisted states are obtained in the absence of heterogeneity ($0 \leq t < 1000$). However, as expected, any of q -twisted states except for the target one, $q = 1$, are broken down by turning on the frequency heterogeneity ($1000 \leq t \leq 3000$). The target twisted state persists even after the heterogeneity is removed ($t > 3000$).

IV. SUMMARY AND DISCUSSION

We have investigated a population of phase oscillators on a ring and found that the multi-stability of the system critically depends on the phase delay and the frequency heterogeneity, controlled by the parameters $0 \leq \alpha < \frac{\pi}{2}$ and $\sigma > 0$, respectively. As α increases, the basin size of the twisted states with larger $|q|$ values increases. Thus, steeper wave-like patterns are more frequently obtained for larger α values. The most robust state against frequency heterogeneity depends on the frequency set $\{\hat{\omega}_k\}$ and α . Statistically, q of the most robust state is 0 for $\alpha = 0$ and increases with α . As σ increases, twisted state with q values further from the most robust one disappear first. Utilizing these properties, we proposed a control method to obtain a target twisted state using α and σ as control parameters.

Understanding basin sizes is an important issue in nonlinear dynamical systems. Generally speaking, the basin size is determined by the nonlinearity of a system and its theoretical quantification is challenging in most systems. This is the case in our system as well. Even for $\alpha = \sigma = 0$, the basin size has been investigated mostly numerically^{13–15}. We expected that linear stability might give some clues at least

about α -dependence, but it did not help. Since both α - and σ -dependence are important in applications, further theoretical exploration would be of great significance.

ACKNOWLEDGMENTS

This study was supported by the JSPS KAKENHI (Nos. JP21K12056, JP22K18384, and JP23H02796) to H.K.

- ¹A. T. Winfree, “Biological rhythms and the behavior of populations of coupled oscillators,” *Journal of theoretical biology* **16**, 15–42 (1967).
- ²Y. Kuramoto, *Chemical Oscillations, Waves, and Turbulence* (Springer-Verlag Berlin Heidelberg, 1984).
- ³A. T. Winfree, *The geometry of biological time* (Springer-Verlag New York, 2001).
- ⁴A. Pikovsky, M. Rosenblum, and J. Kurths, *Synchronization: a universal concept in nonlinear sciences* (Cambridge University Press, 2001).
- ⁵J. Buck, “Synchronous rhythmic flashing in fireflies. ii.” *Q. Rev. Biol.* **63**, 265 (1988).
- ⁶I. Aihara, T. Mizumoto, T. Otsuka, H. Awano, K. Nagira, H. G. Okuno, and K. Aihara, “Spatio-temporal dynamics in collective frog choruses examined by mathematical modeling and field observations,” *Scientific reports* **4**, 3891 (2014).
- ⁷R. Cossart, D. Aronov, and R. Yuste, “Attractor dynamics of network up states in the neocortex,” *Nature* **423**, 283–288 (2003).
- ⁸P. J. Menck, J. Heitzig, J. Kurths, and H. J. Schellnhuber, “How dead ends undermine power grid stability,” *Nature communications* **5**, 3969 (2014).
- ⁹L. Glass, “Multistable spatiotemporal patterns of cardiac activity,” *Proceedings of the National Academy of Sciences* **102**, 10409–10410 (2005).
- ¹⁰D. Bucher, G. Haspel, J. Golowasch, and F. Nadim, “Central pattern generators,” *eLS*, 1–12 (2015).
- ¹¹K. L. Briggman and W. Kristan Jr, “Multifunctional pattern-generating circuits,” *Annu. Rev. Neurosci.* **31**, 271–294 (2008).
- ¹²C. C. Canavier, D. A. Baxter, J. W. Clark, and J. H. Byrne, “Control of multistability in ring circuits of oscillators,” *Biological cybernetics* **80**, 87–102 (1999).
- ¹³D. A. Wiley, S. H. Strogatz, and M. Girvan, “The size of the sync basin,” *Chaos: An Interdisciplinary Journal of Nonlinear Science* **16** (2006).
- ¹⁴R. Delabays, M. Tyloo, and P. Jacquod, “The size of the sync basin revisited,” *Chaos: An Interdisciplinary Journal of Nonlinear Science* **27** (2017).
- ¹⁵Y. Zhang and S. H. Strogatz, “Basins with tentacles,” *Physical Review Letters* **127**, 194101 (2021).
- ¹⁶H. Sakaguchi and Y. Kuramoto, “A soluble active rotator model showing phase transitions via mutual entertainment,” *Progress of Theoretical Physics* **76**, 576–581 (1986).
- ¹⁷H. Sakaguchi, S. Shinomoto, and Y. Kuramoto, “Mutual Entrainment in Oscillator Lattices with Nonvariational Type Interaction,” *Prog. Theo. Phys.* **79**, 1069 (1988).
- ¹⁸B. Blasius and R. Tönjes, “Quasiregular concentric waves in heterogeneous lattices of coupled oscillators,” *Phys. Rev. Lett.* **95**, 84101 (2005).

Appendix A: stability analysis of uniformly twisted states

Here, we conduct the stability analysis of the uniformly twisted states, given by Eq. (2), for Eq. (3) with $\omega_k = 0$ (i.e., without frequency heterogeneity). We describe the state as

$$\phi_k = \Omega t + \frac{2\pi q k}{N} + \xi_k, \quad (\text{A1})$$

where $\Omega = 2 \sin \alpha \cos \frac{2\pi q}{N}$ and ξ_k is a small deviation from the the uniformly twisted state. By substituting this into Eq. (3), we obtain

$$\dot{\xi}_k = \sin \left(\frac{2\pi q}{N} + \xi_{k-1} - \xi_k + \alpha \right) + \sin \left(-\frac{2\pi q}{N} + \xi_{k+1} - \xi_k + \alpha \right) - 2 \sin \alpha \cos \frac{2\pi q}{N} \quad (\text{A2})$$

$$= \sin \left(\frac{2\pi q}{N} + \alpha \right) \cos(\xi_{k-1} - \xi_k) + \cos \left(\frac{2\pi q}{N} + \alpha \right) \sin(\xi_{k-1} - \xi_k) \quad (\text{A3})$$

$$+ \sin \left(-\frac{2\pi q}{N} + \alpha \right) \cos(\xi_{k+1} - \xi_k) + \cos \left(-\frac{2\pi q}{N} + \alpha \right) \sin(\xi_{k+1} - \xi_k) - 2 \sin \alpha \cos \frac{2\pi q}{N}. \quad (\text{A4})$$

By linearizing the equation for small ξ_k , we obtain

$$\dot{\xi}_k = \cos \left(\frac{2\pi q}{N} + \alpha \right) (\xi_{k-1} - \xi_k) + \cos \left(-\frac{2\pi q}{N} + \alpha \right) (\xi_{k+1} - \xi_k). \quad (\text{A5})$$

The stability of this linear equation can be found by substituting the following expression into Eq. (3):

$$\xi_k = e^{\lambda_p t + \frac{2\pi p}{N} k}, \quad (\text{A6})$$

where p ($p = 0, 1, \dots, N-1$) is the wave number of the perturbation and λ_p is the eigenvalues of the stability matrix for the q -twisted state. As a result, we obtain

$$\lambda_p = -2 \left\{ \cos \alpha \cos \frac{2\pi q}{N} \left(1 - \cos \frac{2\pi p}{N} \right) + i \sin \alpha \sin \frac{2\pi q}{N} \sin \frac{2\pi p}{N} \right\} \quad (\text{A7})$$

Trivially, $\lambda_0 = 0$, which exists because of the translational symmetry of the system. If the real parts of the remainder eigenvalues are all negative, then the q -twisted state is stable. This is the case for $-\frac{\pi}{2} < \alpha < \frac{\pi}{2}$ and $|q| < \frac{N}{4}$. For $\frac{\pi}{2} < |\alpha| < \pi$, the q -twisted state with $\frac{N}{4} < |q| < \frac{N}{2}$ are stable. From Eq. (A7), it is clear that the real part is proportional to $\cos \alpha$, thus for any α , the ratio between the real parts of the eigenvalues of two different q -twisted states are the same.